ATLAS calorimeter performance at low p_T for γ, π^0 and η particles identification in the B-physics context

F. Ohlsson-Malek, M. Melcher

ATLAS Internal Note
ATL-COM-PHYS-2001-021
ISN-01.75
September 10^{th}, 2001.

ATLAS Calorimeter performance at low p_{T} for γ, π^0 and η particles identification in the B-Physics Context

F. Ohlsson-Malek [1], M. Melcher

Institut des Sciences Nucléaires, Université J. Fourier,
IN2P3-CNRS, F-38026 Grenoble, France

Abstract

In ATLAS CP violation is studied in the B meson decays. Some of the decay modes are subject to an extensive study in the liquid argon calorimeter such as B_s decay to $J/\psi\ \eta$ where the η particle decays to two γ's and $B_d \to J/\psi\ K^{*0}$ where the K^{*0} decays to $K^0\pi^0$. The observability of these channels is subject to the capability of the calorimeter to detect the low p_{T} clusters produced from the decay of η and π^0 particles to two γ's . It is also important to clean up the data from the electronic noise and the pile-up effects since this latter produces mostly soft charged and neutral pions.

One can achieve an η detection efficiency of about 2.26% with an amount of fake rate of about 24% which makes the study of $B_s \to J/\psi\,\eta$ feasible. A π^0 detection efficiency of 9% is obtained but the fake rate amounts to 73%. Subsequently, it is shown that $B_d \to J/\psi\ K^{*0}$ mode is rather difficult to study.

[1] fmalek@isn.in2p3.fr

1 Introduction and Motivations

CP violation is still one of the experimentally least constrained phenomena in the Standard Model description of electroweak interactions. A very fruitful testing ground for this, is the exploration of Physics with b-flavoured hadrons. At hadron machines, like the LHC, very precise measurements of CP violation can be done and clear answers on the validity of the Standard Model and the existence of New Physics will be achieved.

The B_s decay to $J/\psi\ \eta$ is a mode similar to B_s decay to $J/\psi\ \phi$ (golden decay mode for the B_s meson) with an upper limit branching ratio of $3.8 \cdot 10^{-3}$. Therefore, we expect small CP-violation effects within the Standard Model and New Physics contributions to $B_s \bar{B_s}$ mixing, leading to large CP asymmetries. The B_s decay to $J/\psi\ \eta$ is a pure CP eigenstate decay. As a consequence, there is no need to perform heavy angular analysis to distinguish between final states as it will be the case for the $J/\psi\ \phi$ decay. Similarily to the work presented for $B_{d,s} \to J/\psi\ K_s$ in [1], it has been proposed to extract the angle γ of the Unitarity triangle through measurements of CP asymmetries in the $B_d \to J/\psi\ \eta$ process and measurements of the CP averaged widths of the $B_{d,s} \to J/\psi\ \eta$ processes [2].

Arguments in favour of the measurement of $B_d \to J/\psi\ K^{*0}$ decay mode are numerous. It has a branching ratio of $(1.58 \pm 0.27) \cdot 10^{-3}$, interesting compared to the golden plated mode ($B_d \to J/\psi\ K_s$) branching ratio of $5.\ 10^{-4}$. Similarily to this later mode, it can measure the CP asymmetry, help to extract the β Unitarity angle and probe the accuracy of the Standard Model. Let us remind that K^{*0} decays to $(K^0 \to K_s, \pi^0)$ and that $B_d \to J/\psi\ K^{*0}$ is not a pure final CP eigenstate mode. Fortunately, final states with different CP quantum numbers can be separated by measuring angular distributions.

The observability of these channels is subject to the capability of the calorimeter to detect the low p_{T} clusters produced from the decay of η and π^0 particles to 2 γ's . It is also important to distinguish between clusters produced from single photons and those produced from the two γ's decays which end superimposed onto 1 cluster in the calorimeter. We need also to distinguish between η and π^0 particles and to clean the data from the electronic noise and the pile-up effects since this latter produces mostly soft charged and neutral pions.

The Liquid Argon Calorimeter particle identification power is studied in the offline analysis level.

2 Data samples and Analysis

We study the exclusive modes $B_s \to J/\psi\eta$ and $B_d \to J/\psi K^{*0}$. At the generation level, the $J/\psi \to \mu^+\mu^-$ decay was forced. The decays $\eta \to \gamma\gamma$

and $K^{*0} \to K^0 X$ ($K^0 \to K_s$) were selected. The $K^{*0} \to K^0\ \pi^0$ branching rate ist next to 100%, but also a few $K^{*0} \to K^0\ \gamma$ decays appear [6]. The LVL1 cuts ($P_T(\mu) > 6$ GeV/c, $|\eta\,^2| < 2.5$) were also applied at the generation level. The event generation is performed using PYTHIA version 5.7 [3] where we chose the production of $b\bar{b}$, forcing $\bar{b}$ to decay to $J/\psi\eta$ (respectively to $J/\psi K^{*0}$). The sets of data were used as inputs for a full simulation in the ATLAS detector using the ATLAS Geant3 based program DICE, srt release 1.3.0. The reconstruction was performed using the ATLAS program ATRECON, srt release 1.3.0. A total of 17000 (respectively 20000) fully simulated and reconstructed $B_s \to J/\psi\eta$ (resp. $B_d \to J/\psi K^{*0}$) events were obtained. Three samples of about 10000 single particles (η, γ, π^0) have also been used for the detailed study of the particle identification and to perform efficient cuts for pile-up rejection. The Combined Ntuples (CBN-Tuples) [5] facility was used for analysis with PAW and ROOT.

In the Electromagnetic CALorimeter (ECAL), a cluster is defined as the energy deposit inside the region $\Delta\eta \times \Delta\phi$ =0.075 x 1.25, which corresponds to 3x5 cells in the 2nd sampling. To find clusters candidates the cells of the different samplings are mapped onto towers of size 0.025x0.025 and a sliding window algorithm is used, taking a 3x3 towers and a transverse energy threshold of 1 GeV. The electronic noise and the pile-up were added at the reconstruction level as described in [4].

An algorithm based on the selection of the two clusters of highest transverse energies was applied to build the clusters invariant mass using their kinematical characteristics ($\mathrm{E}_{cluster}$, $\eta_{cluster}$ and $\phi_{cluster}$). Only 20% of the generated η particles decaying into two γ's have a $\gamma\gamma$ opening angle higher than 5° and a γ energy higher than 1 GeV. Therefore, the η detection efficiency will be limited to 20% due to the resolution of the ECAL and the clusterization conditions.

Another algorithm has been built to collect events where the shower of the two γ's from the η decay are overlapping and which are reconstructed as one cluster in the ECAL. This is also the case for the π^0's where most events, due to the small $\gamma\gamma$ opening angle, give 1 cluster.

For the following analysis, only the ten electromagnetic clusters with highest transverse energy are taken into account.

In order to obtain reconstruction efficiencies and the fake rates, the reconstructed particles had to be identified with the generation data, the 'truth'. For this, the direction of the generated particle and the direction of the reconstructed one were compared. A reconstructed particle was said to be a true particle, if a generated particle satisfying

$$\angle\ (\vec{p}_{generated}, \vec{p}_{reconstructed}) < 2^\circ \tag{2.1}$$

[2]Throughout this paper, the symbol η is used for the pseudorapidity as well as for the particle itself

was found. When there were more than one true particle satisfying this relation, the particle with the closest angle was selected.

3 Definitions: Efficiency and fake rate

The main criteria for judging the reconstruction quality are the reconstruction efficiency and the fake rate, defined as follows:

- N_X: Number of reconstructed X particles
- N_X^{true}: Number of reconstructed X particles associated to a generated X particle
- N_X^{fake}: Number of reconstructed X particles not associated to a generated X particle: $N_X = N_X^{true} + N_X^{fake}$
- N_X^{gen}: Number of generated X particles
- $N_{X\ from\ Y}^{true}$: Number of reconstructed particles associated to a generated X particle belonging to the decay channel Y
- $N_{X\ from\ Y}^{gen}$: Number of generated X particles belonging to the decay channel Y
- Overall X reconstruction efficiency:

$$\epsilon(X) = \frac{N_X^{true}}{N_X^{gen}} \tag{3.1}$$

- X from Y efficiency

$$\epsilon(X\ from\ Y) = \frac{N_{X\ from\ Y}^{true}}{N_{X\ from\ Y}^{gen}} \tag{3.2}$$

- fake rate :

$$f_X = \frac{N_X^{fake}}{N_X} \tag{3.3}$$

4 η reconstruction

4.1 The visibility

The main criterium for η identification is the invariant mass of the two γ particles. Hence, for the reconstruction to be possible, two separated clusters are required. Therefore, the following two conditions have to be satisfied:

η particles decaying into two γ...	All η	η from B_s
(1) pointing to two clusters	1967 $\hat{=}$ 12.7%	1809 $\hat{=}$ 14.5%
(2) pointing to the same cluster (superimposition)	447 $\hat{=}$ 2.9%	428 $\hat{=}$ 3.4%
(3) One pointing to a cluster, one without cluster	5028 $\hat{=}$ 32.4%	4765 $\hat{=}$ 38.1%
(4) Not pointing to any cluster	8060 $\hat{=}$ 52.0%	5516 $\hat{=}$ 44.1%
Total	15502	12518

Table 1: η visibility

- The $\gamma\gamma$ opening angle has to be high enough ($> 5°$) so that the clusters in the ECAL are not superimposed.
- The γ energies have to be sufficient ($p_T > 1$ GeV) for the cluster to be found by the clusterization algorithm.

The ratio of η particles satisfying these two conditions gives an upper limit to the reconstruction efficiency which can be achieved by the method presented here. As shown in table 1, the maximum reconstruction efficiency that can be achieved is 14.5%. Most of the η particles are lost because the energy of at least one of the γ particles is less than 1 GeV.

4.2 Reconstruction without pile-up

The distribution of the invariant mass for all possible two-cluster-pairs, figure 1(a), shows the eta peak above the combinatorial background. In order to suppress this combinatorial background, we only look at the two clusters of highest transverse energy. Choosing the clusters by total energy (instead of transverse energy) was shown to give worse results (smaller efficiencies and higher fake rates). The resulting invariant mass distribution is plotted in figure 1(b). 4.0% of the η particles from B_s decays were found in an invariant mass window of $\pm 2\sigma$ around the η mass (0.547 GeV [6]), but still 42% of the reconstructed η are fakes. The parameters of the gauss-fit and the obtained efficiencies are summed up in table 3 (left side).

For all the following analysis, an invariant mass window of $\pm 2\sigma$ will be used.

4.3 Reconstruction with pile-up

With pile-up at low luminosity and the electronic noise, lots of clusters not originating from η but from other particle decays appear as background noise, as can be seen in figure 2(a). As only two clusters per event are taken

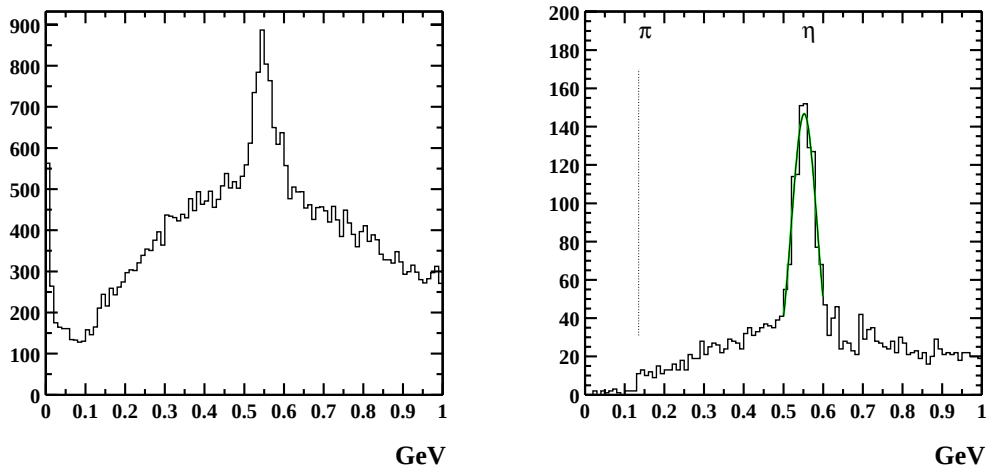

(a) Data without pile-up, combinatorial

(b) Data without pile-up, no cuts

Figure 1: Two clusters invariant mass. (a) combinatorial, (b) 2 clusters of highest p_{T}, no pile-up and no cuts.

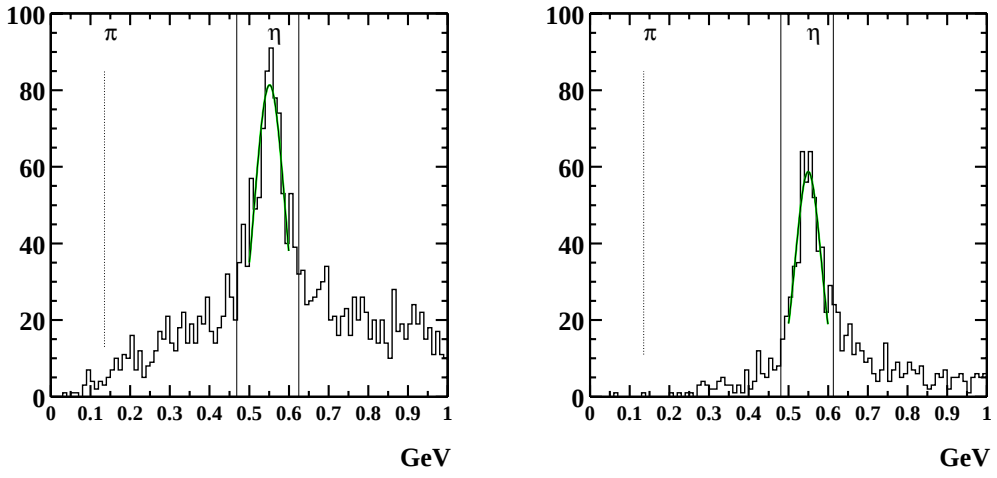

(a) Data with pile-up, no cuts

(b) Data with pile-up, cuts applied

Figure 2: 2 clusters invariant mass: 2 clusters of highest p_T, with gauss fit on the η peak and $\pm 2\sigma$ invariant mass window shown by the horizontal lines

into account, each cluster not originating from the η decay may hide an η cluster. Consequently, the reconstruction efficiency falls to 2.9%, while the fake rate increases to 45%. The detailed results are summed up in table 3 (right side).

Using the generation data, the real origins of clusters which were identified as γ from η (in the 2σ invariant mass window) were searched for. As listed up in table 2, the main contributions are coming from charged and neutral pions, photons and noise.

η	785	$\hat{=}$	72%
π^0	46	$\hat{=}$	5%
$\pi^{\pm}$	30	$\hat{=}$	3%
γ	116	$\hat{=}$	11%
other particles and noise	102	$\hat{=}$	9%

Table 2: Origin of clusters being identified as γ from η (2σ invariant mass window)

The task is now to suppress everything that doesn't originate from real η decays.

4.4 Cluster rejection

Clusters originating from hadrons or noise can be identified and rejected using geometrical properties of the cluster:

- In order to reject background photons, which are situated at low p_T, and the electronic noise, clusters were rejected if the transverse energy is less than 2 GeV. As the photons from η are also situated at rather low p_T, this cut alone reduces significantly the η reconstruction efficiency.
- In the ECAL, hadrons are not absorbed as easily as $e^{\pm}$ and γ particles. Therefore, they deposit a higher part of their energy in the third sampling of the ECAL and in the first sampling of the hadronic calorimeter. Therefore, clusters were rejected if more than 4% of the total energy is deposited in the third sampling or if more than 10% of the total transverse energy is deposited in the first sampling of the HCAL, see figures 3(a) and 3(b).
- Clusters originating from photons are thinner than hadronic clusters, including clusters from π^0, which are the superimposition of two photons with slightly different directions. Therefore, clusters were rejected if the total cluster width, calculated using the energy deposition in 40 strips of the first sampling, is larger than 8 strips, see figure 3(c).
- Still taking profit of the difference in the cluster width, cuts on the energy leakage were applied: In photonic clusters, most of the energy

η reconstruction without pile-up	
$\#events$	17039
N_{η}^{gen}	20795
$N_{\eta\ from\ B_s}^{gen}$	17094
N_{η}	1164
N_{η}^{true}	684
$N_{\eta\ from\ B_s}^{true}$	676
$\epsilon(\eta\ from\ B_s)$	4.0%
f_{η}	42%
Gaussfit mean	0.552 GeV
Gaussfit σ	0.032 GeV

η reconstruction with pile-up	
$\#events$	16697
N_{η}^{gen}	20368
$N_{\eta\ from\ B_s}^{gen}$	16749
N_{η}	833
N_{η}^{true}	479
$N_{\eta\ from\ B_s}^{true}$	475
$\epsilon(\eta\ from\ B_s)$	2.9%
f_{η}	45%
Gaussfit mean	0.551 GeV
Gaussfit σ	0.039 GeV

Table 3: Reconstruction efficiencies without cuts, data without and with pile-up. For the definition of the given numbers see section 3 on page 4.

is deposited in a 3x3 cells region in the second sampling. E_{33} being the energy deposited in this 3x3 window of the second sampling, E_{37} the energy deposited in a 3(η dir.)x7(ϕ dir) window and E_{77} the energy in a 7x7 towers window, clusters were rejected if

$$\frac{E_{37}-E_{33}}{E_{37}} > 20\% \quad \text{or} \quad \frac{E_{77}-E_{37}}{E_{77}} > 20\% \tag{4.1}$$

thus demanding that less than 20% of the energy is deposited outside the 3x3 window in both η and ϕ directions, see figure 3(d).

The cuts were applied in such a way that the first two clusters (of highest E_T) passing the cuts were combined for the η reconstruction. While the efficiency fell to 2.26%, as also some real η clusters were rejected, the fake rate could be lowered to 24%. In the obtained invariant mass distribution, as shown in figure 2(b), next to all the noise has disappeared. The detailed reconstruction results are shown in table 4 and the definition of the variables used in table 5. If we use the same cuts on the data without pile-up, the η reconstruction efficiency is found to be equal to 3.28% while the fake η rate is equal to 20%. Therefore, the pile-up is seen to decrease significantly the reconstruction efficiency while it does not increase the fake rate so much.

4.5 $\eta \to 1\ cluster$ events

As listed up in table 1, in some of the η particle decays the $\gamma\gamma$ opening angle is so small that the two clusters are superimposed and identified as a single cluster by the reconstruction software. As it is not possible to calculate an invariant mass for a single cluster, other η selection criteria were searched for. Using the cluster properties provided by the reconstruction software, some cuts could be found which reject a certain number of non-η clusters:

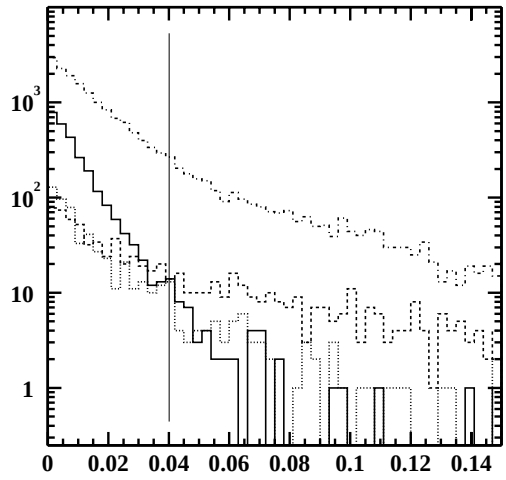

(a) $E(3^{rd} sampling)/E$

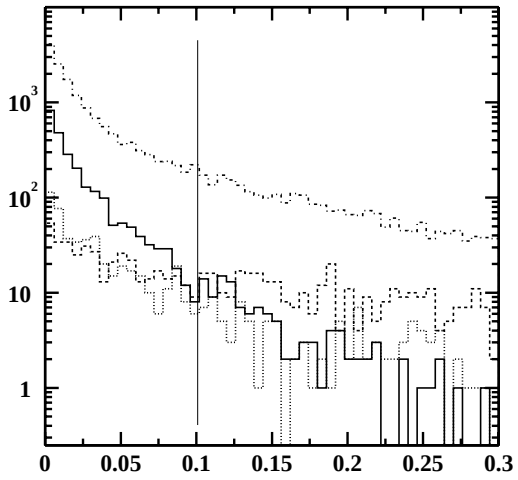

(b) $E_T(1^{st}$hadronic sampling$)/E_T$

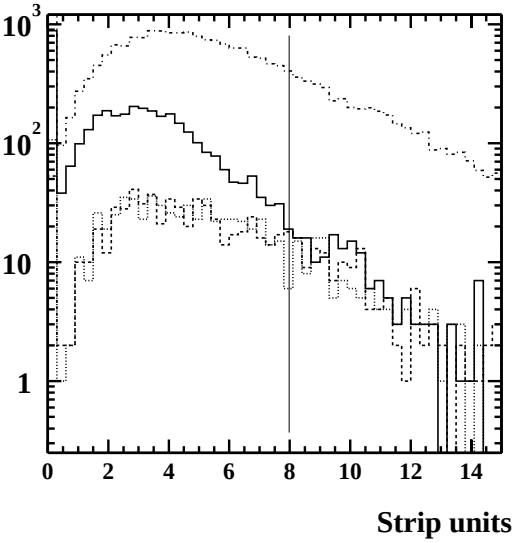

(c) Total cluster width

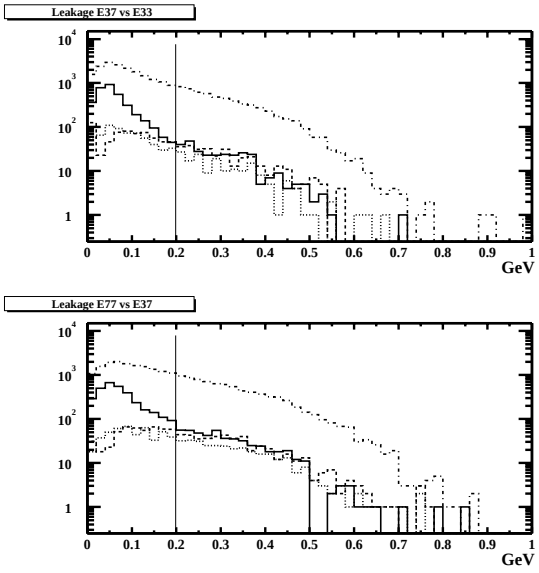

(d) Energy leakage in η(top) and ϕ direction

Figure 3: Cluster properties for clusters from η (–), $\pi^{\pm}$ (– –), $\pi^0(\cdots)$ and the rest $(-\cdot-)$, as well as applied cuts (vertical lines). Only two clusters of highest E_T of each event are considered.

Final cuts for η from B_s selection		
E_T	$>$	2. GeV
$\frac{E3_{35}}{E_{35}}$	$<$	4 %
$\frac{Etha1}{E_T}$	$<$	10 %
$Wtots1$	$<$	8. strips
$\frac{E_{37}-E_{33}}{E_{37}}$	$<$	20 %
$\frac{E_{77}-E_{37}}{E_{77}}$	$<$	20 %

η reconstruction with pile-up	
$\#events$	16697
N_η^{gen}	20368
$N_{\eta\ from\ B_s}^{gen}$	16749
N_η	461
N_η^{true}	371
$N_{\eta\ from\ B_s}^{true}$	367
$\epsilon(\eta\ from\ B_s)$	2.26%
f_η	24%
Gaussfit mean	0.55 GeV
Gaussfit σ	0.033 GeV

Table 4: (Left side)Summary of final cuts applied for the η selection; (right side) Reconstruction efficiencies after cut application, data with pile-up.

E_{35}	Total Energy in the ECAL (3x5 cell)
E_T	Transverse Energy in the ECAL (3x5 cell)
$Wtots1$	Total cluster width (over 40 strips)
$E3_{35}$	Energy in third sampling of the ECAL (3x5 cell)
$Etha1$	ET in first sampling of HAD calorimeter

Table 5: Variables used for η selection

- The transverse energy has to be at least 10 GeV. This rejects most of the pile-up clusters. As the clusters now contain the energy of both γ particles, the typical cluster energy is much higher than in 2 cluster decays.
- The total cluster width (over 40 strips) has to be between 2 and 9 strips. It was shown that most of the η clusters have a width within this window.
- Due to the high pseudorapidity resolution in first sampling, two energy maxima are found corresponding to the two γ, enclosing an energy minimum in between. Clusters were rejected, if this energy minimum is more than 0.4% of the total transverse energy.
- The energy leakage in η and ϕ directions are correlated. Clusters were rejected, if $(E_{37}-E_{33})/E_{37} > 15\%$ and $(E_{77}-E_{37})/E_{77} > 15\%$. Also, clusters were rejected if $(E_{37}-E_{33})/E_{37} > 50\%$ or $(E_{77}-E_{37})/E_{77} > 50\%$. This corresponds to a selection of the clusters inside the frame shown in figure 4.

These cuts were chosen after a comparative analysis of the cluster properties, showing that the typical η clusters would pass the cuts. The obtained

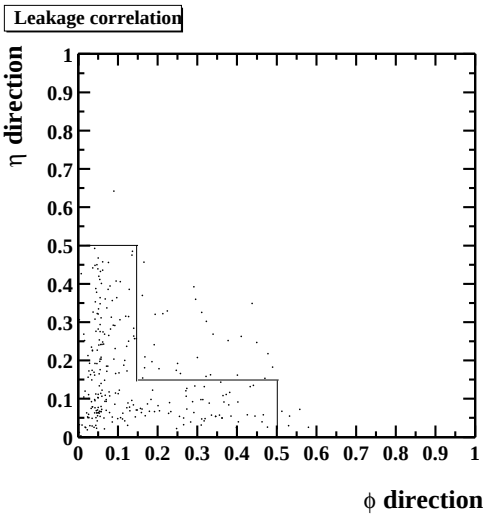

Figure 4: Energy leakage in η and ϕ direction of $\eta \to 1$ *cluster* events and applied cut. See comments in text page 10, third bullet.

$\#events$	16697
N_{η}^{gen}	20368
$N_{\eta \to 1\ cluster}^{gen}$	477
$N_{\eta \to 1\ cluster}$	1073
$N_{\eta \to 1\ cluster}^{true}$	166
$\epsilon(\eta \to 1\ cluster)$	35%
$f_{\eta \to 1\ cluster}$	85%

Table 6: $\eta \to 1$ *cluster* reconstruction with pile-up

efficiencies are shown in table 6.

Here (and only here), for the η identification with the truth, the cluster energy was forced to be within a window of $\pm 30\%$ around the generated η particle energy. As before, the direction of cluster and generated particle had to match within 2°.

The Reconstruction efficiency and the fake rate were not affected by pile-up, because the cluster energies are now superior to the energies of clusters coming from pile-up.

Nevertheless, the obtained fake rate was very high (85%), while the $\eta \to 1$ *cluster* efficiency was 35%, much higher than the $\eta \to 2$ *cluster* efficiency.

Due to the high fake, $\eta \to 1$ *cluster* events are not considered for the B_s reconstruction.

$\#events$	16679		
$\#\gamma$	25370		
$\#\gamma \rightarrow 1$ *cluster*	9369	$\hat{=}$	36.9%
# converted γ	675	$\hat{=}$	2.7%
# converted γ, still giving 1 cluster	361	$\hat{=}$	1.4%
# converted γ, no cluster in γ dir.	314	$\hat{=}$	1.2%

Table 7: Reconstructed photon conversions. Only photons from the decay channel $B_s \rightarrow J/\psi\ \eta\ (\eta \rightarrow \gamma\gamma)$ were counted.

4.6 Conversions in the inner detector

In the inner detector, approx. 20% of the photons convert into e^+/e^--pairs. Depending on the radius where the conversion takes place, some of the clusters from the e^+/e^- are separated (not superimposed) and deviated from the original photon direction by the applied magnetic field. In this case, the photon cannot be found using only the ECAL data. However, photon conversions can be reconstructed using inner detector tracks.

The number of reconstructed photon conversions for photons from $B_s \rightarrow J/\psi\ \eta(\eta \rightarrow \gamma\gamma)$ is shown in table 7.

The algorithm used to take into account the conversions for the η reconstruction tries the following combinations, until an invariant mass within the $\pm 2\sigma$ is found:

1. Two ECAL clusters of highest E_T
2. ECAL cluster of highest E_T and conversion of highest p_T
3. Two conversions of highest p_T

In order to suppress fake conversions, conversions were rejected if the χ^2 fit parameter was superior to 5, value taken arbitrarily. Cluster rejection was not changed.

Taking into account the conversions, the η from B_s efficiency slightly rises from 2.26% to 2.4%, whereas the fake rate rises a little bit. Therefore, the conversions were not considered for the B_s reconstruction, too.

4.7 Consequences for $B_s \rightarrow J/\psi\ \eta$ reconstruction

Without pile-up, we can easily find the η peak at 0.547 GeV when calculating the two clusters invariant mass. The combinatorial background can be mostly eliminated by combining only the two clusters of highest transverse energy. The efficiency of η reconstruction for η particles from B_s decays is 4.0%. When adding pile-up at low luminosity, this efficiency falls to 2.9%, due to clusters originating from soft charged and neutral pions, as well as large amount of photons (not originating from η), small quantities of other

particles (such as electrons and positrons) and electronic noise. They are also responsible for the rather huge fake rate (45%). The pions can be suppressed by applying cuts on the energy deposited in the 3^{rd} EM-sampling and the 1^{st} HCAL sampling, on the cluster width and on the energy leakages in η and ϕ directions. Electronic noise and a part of the photon contribution can be eliminated by applying a 2 GeV transverse energy cut. An η from B_s efficiency of 2.26% was achieved. The fake rate being at 24%, the signal is rather clean.

$\eta \rightarrow 1$ *cluster* events are uninteresting for the reconstruction, as the clusters cannot be easily identified.

As we are at low E_T, only few photon conversions into $e^{\pm}$-pairs were reconstructed. Consequently, adding conversions to the analysis doesn't change the reconstruction efficiency by much and gives a higher fake rate.

After having applied the reconstruction algorithm (without 1 cluster events and conversions) on the physical background, consisting of $B \rightarrow J/\psi\ X$ events, the significance of the signal, which is a measure for the cleanliness, was calculated. The signal was found to be visible enough for the physics analysis [7, 8] since the significance was of the order of 100.

5 K^{*0} reconstruction

The reconstruction of the decay channel $K^{*0} \rightarrow K^0\pi^0(K^0 \rightarrow K^0_s \rightarrow \pi^+\pi^-)$ consists of two tasks: K^0_s reconstruction by identifying the $\pi^{\pm}$ pairs (in the inner detector) and π^0 reconstruction (in the ECAL). For this work, the focus was drawn to the π^0 reconstruction; in order to decide wether an inner detector track came from a $\pi^{\pm}$, the truth was used. Still, for the reconstruction, the measured momentum and direction were used.

5.1 π^0/γ separation

The $\gamma\gamma$ opening angle of $\pi^0 \rightarrow \gamma\gamma$ decays is so small that next to all π^0 give only one cluster in the ECAL, as the clusters from the two photons are superimposed. Therefore, some criteria for π^0/γ separation had to be found. In order to do this, a set of fully simulated single π^0 and single γ events without electronic noise and pile-up was used and the cluster properties were analyzed and compared. The transverse energy given to the π^0's/photons was varied from 1 to 30 GeV; the transverse energy of the resulting clusters is shown in figure 5(a).

As the π^0 clusters are the superimposition of two photon clusters with slightly different directions, the following convention can be used for a differentiation:

- Cluster shape: π^0 clusters are larger than single photon clusters. For this reason, the total cluster width can be used as a selection criterium,

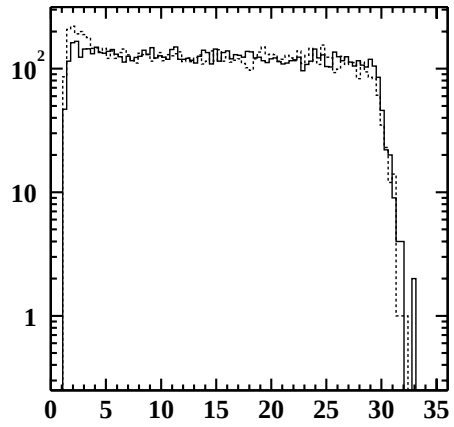

(a) Transverse energy in GeV as measured in ECAL

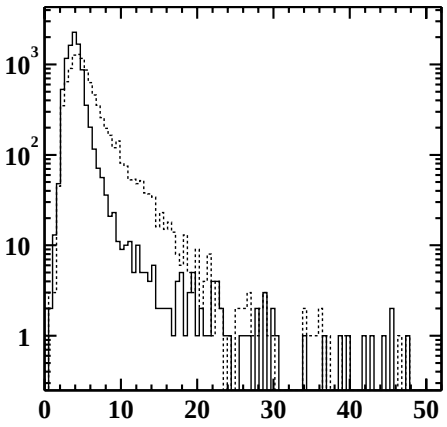

(b) Width(40 strips)/Width(3 strips)

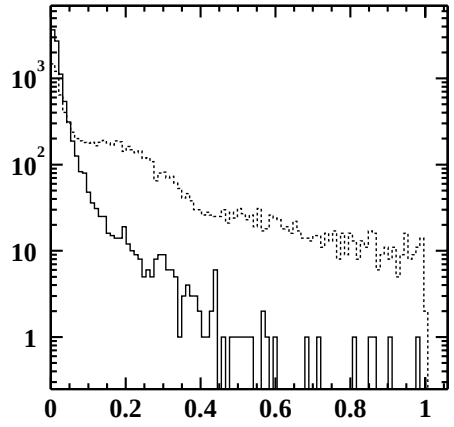

(c) $E_T(2^{nd}\ max\ in\ 1^{st}\ sampl.)/E_T(1^{st}\ sampl.)$

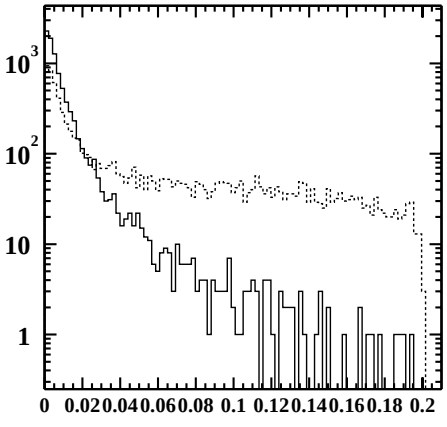

(d) $\frac{E(2^{nd}\ max\ in\ 1^{st} sampl.) - E(min.btw.2\ maxima)}{E_T(1^{st}\ sampl.)}$

Figure 5: Cluster properties for clusters from γ and π^0 (dashed line) : Study from a sample of simulated single π^0 and single γ events without pile-up.

Cuts applied	**Surviving π^0 rate**	**Surviving γ rate**
$\frac{E2tsts1}{E1_{35}/\cosh(\eta_2)} > 0.06$ $\frac{E2ts1-Emins1}{E1_{35}/\cosh(\eta_2)} > 0.02$	45.0%	4.4%
$Wtots1 > 3$ $\frac{E2tsts1}{E1_{35}/\cosh(\eta_2)} > 0.03$ $\frac{E2ts1-Emins1}{E1_{35}/\cosh(\eta_2)} > 0.015$ $Emins1/E1_{35} > 0.01$ $E2ts1/E1_{35} > 0.02$	22.8%	2.9%

Table 8: π^0/γ separation at $p_T = 0..30$ GeV. The variables are explained in table 9.

$E2tsts1$	Transverse energy of 2nd max (1 strip) in first sampling
$E2ts1$	Transverse energy of 2nd max (3 strips) in first sampling
$Emins1$	Energy minimum between two maxima in first sampling
$Wtots1$	Total cluster width (over 40 strips)
$E1_{35}$	Energy in first sampling (3x5 cell)
η_2	Pseudorapidity as measured in second sampling
$Weta1$	Cluster width (over 3 strips)

Table 9: Variables used for π^0/γ separation

see figure 5(b).

- Second max: The first sampling of the ECAL has a high granularity in the η direction. Therefore, two energy deposition maxima can be identified, corresponding to the two photons, figure 6. Useful information, such as the transverse energy of the second maximum and the minimum between the two maxima is provided by the reconstruction software and can easily be used for differentiation, see figures 5(c) and 5(d).

High photon rejection and acceptable π^0 efficiencies could be achieved by applying simple cuts on the mentioned cluster properties, as shown in table 8.

5.2 π^0 selection

In order to find the π^0 coming from the K^{*0} decay, the ECAL cluster of highest p_T which passes the chosen cuts was selected. Compared to the π^0 studied above, the π^0 concerned here are at lower transverse momentum, and the cuts presented above appear to be next to useless. Additionally, the π^0 we are looking for are energetically rather close to the pile-up as seen on

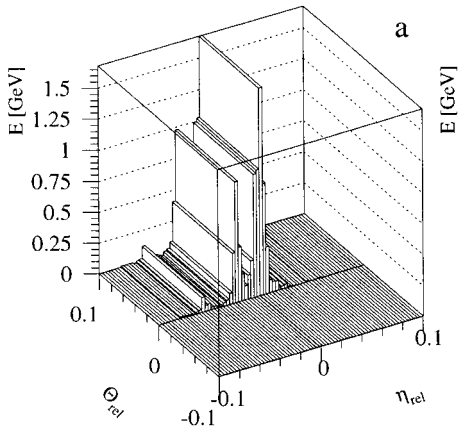

Figure 6: Substructure of a hadronic cluster in the 1^{st} sampling of the ECAL [9]: Two energy maxima are visible

figure 7, wich makes the search even more difficult.

Figure 8(a) shows the correlation between generated and reconstructed transverse momentum: They match within an acceptable range, as the root mean square of $(p_T^{reconstructed} - p_T^{generated})/p_T^{generated}$ was 0.18, as shown in figure 8(b).

The π^0 rejection was optimized in order to obtain the lowest possible fake rate. Table 10 shows the applied cuts and the efficiency obtained: The achieved π^0 from K^{*0} efficiency was 9.0%, while the fake rate was 73%.

The cuts were found by using a simple search algorithm which finds the cut value giving the minimal fake rate, provided that not more than 70% of the real π^0's are rejected. The cuts slightly improve the π^0 fake rate, but the π^0 from $K^{*0}(B_d)$ efficiency has dropped. With and without the cuts applied, approximately the same amount of the real reconstructed π^0 (38%) is not coming from K^{*0} decays.

5.3 K_S^0 reconstruction

For the $K_S^0 \to \pi^+\pi^-$ reconstruction, the inner detector tracks were used for $\pi^\pm$ reconstruction.

Several approaches were made in order to reconstruct the K_S^0 particles. In all cases, the truth (data from generation) was used in order to decide whether a track is coming from a $\pi^\pm$. However, for the reconstruction, the momentum observed by the inner detector was used. In all cases, the inner detector tracks with a fit parameter $\chi^2 > 6$ were rejected. Two of the used methods are presented below

1. **For reference: Use of the simulation truth.** Using the data from generation, the $\pi^\pm$-pairs coming from the $K_S^0(B_d \to J/\psi K^{*0})$ decays

Cuts for π^0 from K^{*0} selection				
		E_T	$>$	2.5 GeV
		$\frac{E_{37}-E_{33}}{E_{37}}$	$>$	0.02
1.8	$<$	$Wtots1$	$<$	7.8
0.04	$<$	$\frac{E2tsts1}{E_{35}/\cosh(\eta_2)}$	$<$	1.44
3.2	$<$	$\frac{Wtots1}{Weta1}$	$<$	16.8
		$\frac{E2tsts1-Emins1}{E_{35}/\cosh(\eta_2)}$	$>$	0.016

π^0 selection with pile-up	
$\#events$	9016
$N^{gen}_{\pi^0}$	60104
$N^{gen}_{\pi^0\ from\ B_d\to J/\psi K^{*0}}$	8963
N_{π^0}	4811
$N^{true}_{\pi^0}$	1300
$N^{true}_{\pi^0\ from\ B_d\to J/\psi K^{*0}}$	805
$\epsilon(\pi^0\ from\ B_d\to J/\psi K^{*0})$	9%
f_η	73.0%

Table 10: π^0 from K^{*0} reconstruction: Applied cuts (left side) and efficiencies (right side). The meanings of the variables are listed up on page 15.

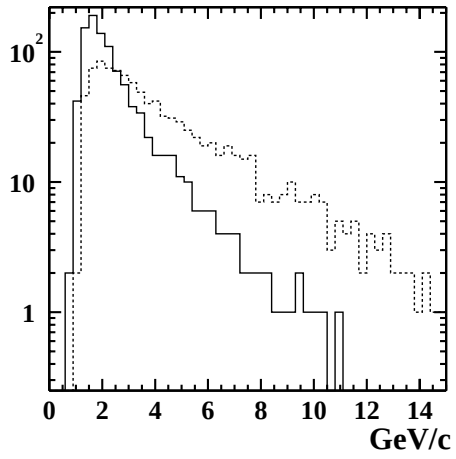

Figure 7: p_{T} of π^0 from K^{*0} and other clusters (- -). Both curves are normalized to 1000 events.

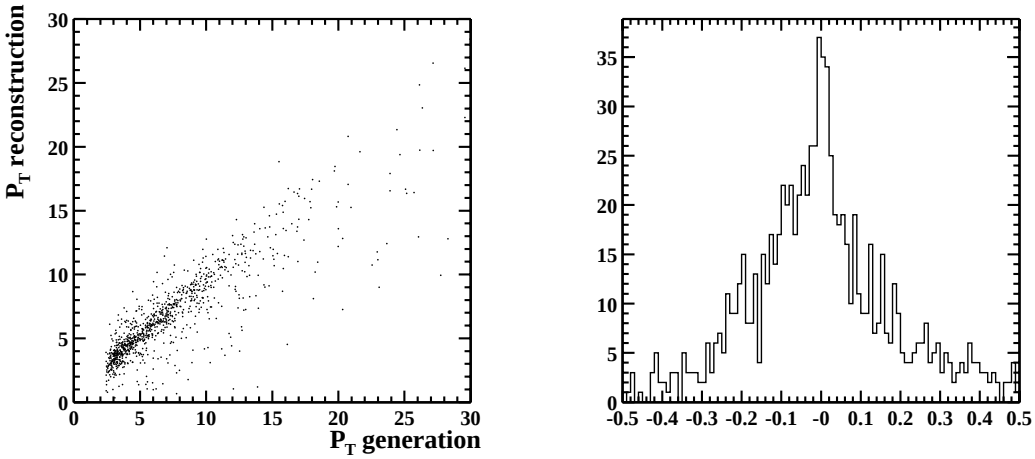

(a) p_{T} from generation (x axis) and reconstructed p_{T} (y axis) for π^0 from K^{*0}, GeV/c units.

(b) $\frac{p_T^{reconstructed} - p_T^{generated}}{p_T^{generated}}$

Figure 8: π^0 from K^{*0} p_{T} from generation and reconstruction

were searched for. Consequently, the K_S^0 fake rate is practically ≈ 0. The K_S^0 from $K^{*0}(B_d)$ efficiency was 31%.

2. **Select $\pi^{\pm}$ with best invariant mass.** Finally, each π^+ was combined with each π^-, and the combination giving the best invariant mass (closest to the K^0 mass) was chosen. The fake rate rises to 85%, and the efficiency drops to 11%.

The detailed results of K_S^0 reconstruction using these two methods are given in table 11. As before, an invariant mass window of $\pm 2\sigma$ was used for all analysis. The invariant mass distributions are shown in figure 9.

An optimized K_S^0 reconstruction method using specific cuts on the tracks and vertexing is described in [10], where an efficiency of 41% was achieved.

5.4 K^{*0} reconstruction

The last step is to combine the reconstructed K_S^0 with the π^0 particles in order to reconstruct the K^{*0} particle. The best results were obtained by combining the best invariant mass method for the K_S^0 with the cuts for the π^0 as described above; The $K_S^0 - \pi^0$ invariant mass distribution is shown in figure 10; the reconstruction results are listed up in table 12. The

K^0_S reconstruction with pile-up	
$\#events$	11274
$N^{gen}_{K^0_S}$	19213
$N^{gen}_{K^0_S\ from\ B_d}$	11274

Using the simulation truth	
$N_{K^0_S}$	3502
$N^{true}_{K^0_S}$	3484
$N^{true}_{K^0_S\ from\ B_d}$	3484
$\epsilon(K^0_S\ from\ B_d)$	31%
$f_{K^0_S}$	0.5%
Gaussfit mean	0.499 GeV
Gaussfit σ	0.057 GeV

$\pi^{\pm}$ with best invariant mass	
$N_{K^0_S}$	9139
$N^{true}_{K^0_S}$	1359
$N^{true}_{K^0_S\ from\ B_d}$	1193
$\epsilon(K^0_S\ from\ B_d)$	11%
$f_{K^0_S}$	85%
Gaussfit mean	0.498 GeV
Gaussfit σ	0.014 GeV

Table 11: $K^0_S \to \pi^+\pi^-$ reconstruction

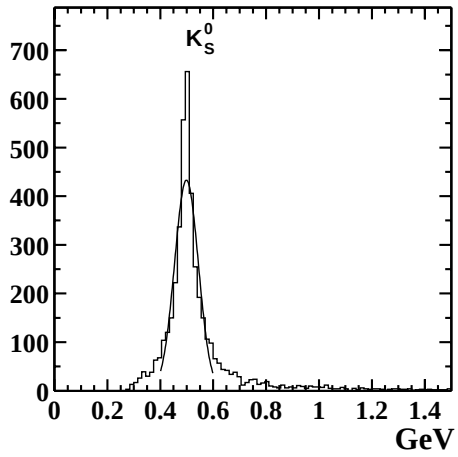

(a) $\pi^+ - \pi^-$ invariant mass: Using the truth

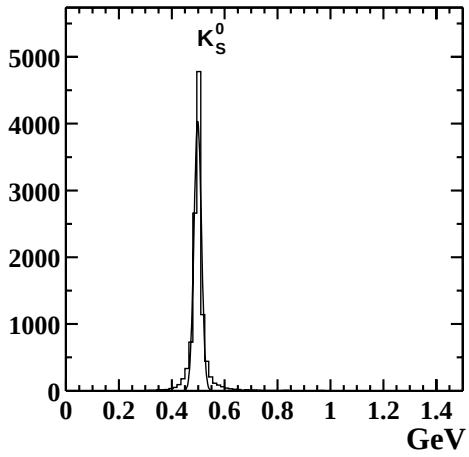

(b) $\pi^+ - \pi^-$ invariant mass: $\pi^{\pm}$ with best invariant mass

Figure 9: K^0_S reconstruction

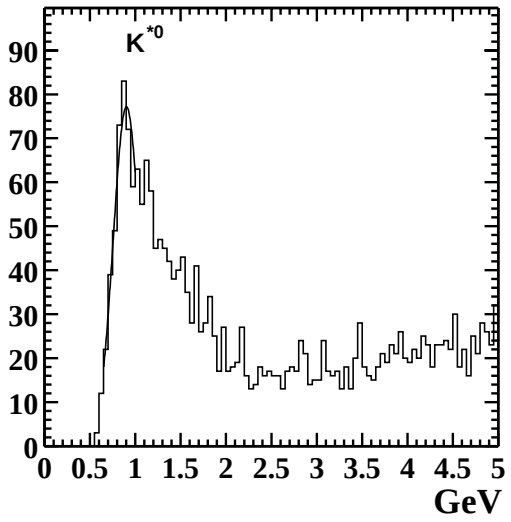

Figure 10: K^{*0} reconstructon: $K^0_S - \pi^0$ invariant mass

obtained efficiency with this method was 1.2% with a fake rate of 75%. If we try to select the π^0 clusters close to the K^0_S momentum direction, we will probably reduce the background and improve the reconstruction efficiency significantly. This task has not been done yet.

5.5 Consequences for $B_d \to J/\psi\ K^{*0}$ reconstruction

Whereas π^0/γ-distinction appears not to pose big problems at higher transverse momentum, no effective distinction criterium could be found which could have helped to identify the neutral pions from K^{*0} decays. Some cuts were found which slightly ameliorate the fake rate but which reject also many real π^0 particles. The cuts had the same impact on the K^{*0} reconstruction: The fake rate dropped by some percent, but a great amount of K^{*0} was lost, too. Table 13 gives a short overview of the K^{*0} efficiencies obtained by the different methods.

It appears that the K^{*0} reconstruction could still be rescued by a better K^0_S reconstruction method, as the K^{*0} fake rate is at a rather low level if the truth is used for the K^0_S, even if the π^0 fake rate is very high. Selecting π^0's only around the K^0_S direction (instead of taking the whole π^0 angular spectrum), might reduce the background significantly, thus improving the reconstruction efficiency. In addition, a big part of the K^{*0} should possibly be suppressed if the combination with the J/ψ particle is done in order to reconstruct the B_d meson.

K^{*0} reconstruction with pile-up	
$\#events$	11274
$N^{gen}_{K^{*0}\ from\ B_d}$	11274
$N_{K^{*0}}$	569
$N^{true}_{K^{*0}}$	139
$N^{true}_{K^{*0}\ from\ B_d}$	137
$\epsilon(K^{*0}\ from\ B_d)$	1.2%
$f_{K^{*0}}$	75%
Gaussfit mean	0.902 GeV
Gaussfit σ	0.147 GeV

Table 12: K^{*0} reconstruction; with pile-up; K^0_S reconstruction using the best invariant mass method; π^0 selection after cut application.

π^0 **selection**	K^0_S **reconstruction**	$K^{*0}(B_d)$ **efficiency**	K^{*0} **fake rate**
no cuts	using the truth	5.0%	12%
no cuts	best inv. mass	2.2%	77%
cuts applied	using the truth	3.0%	11%
cuts applied	best inv. mass	1.2%	75%

Table 13: K^{*0} reconstruction: Summary

Making the most optimistic assumptions, and assuming additionnally that the J/ψ particles can be reconstructed with a good efficiency and a very low fake rate, the upper limit to the B_d signal significance of ≈ 60 can be achieved.

6 Conclusion

The goal of this work was to find strategies to identify low p_T γ, η and π^0 particles from $B_s \to J/\psi\ \eta$ and $B_d \to J/\psi\ K^{*0}$ decays and to give estimates on the reconstruction efficiencies which will be achieved in the ATLAS detector at LHC.

Using cuts on cluster width, energy leakage and energy deposition in the third ECAL and first HCAL sampling, the clusters from $\eta \to \gamma\gamma$ could be identified, rejecting the major part of hadronic jets and noise. An η reconstruction efficiency of 2.26% could be achieved; the ratio of fake η particles being at 24%, the reconstruction can be said to be sufficiently clean. In combination with the J/ψ reconstruction [7, 8], the expected significance of the B_s signal was found to be sufficiently high (≈ 100).

γ/π^0 separation, needed to identify the π^0 particles from K^{*0} decays, seemed to be feasible at high p_T ($\approx 1 - 30$ GeV), using the substructure of

the clusters (second maximum, cluster width). Unfortunately, the π^0 from K^{*0} are at low p_T (some GeV) and energetically at the same level as the pile-up. Therefore, the identification is much more difficult. Nevertheless, a reconstruction efficiency of 9% could be achieved, whereas 73% of the reconstructed π^0 were fakes. Thereby, the measurement of the transverse momentum satisfies the requirements. It was shown that a large part of the fake pions can be rejected by combining them with the K_S particles (K^{*0} reconstruction), using an optimal K_S reconstruction algorithm. Despite the difficulties we encountered for obtaining a clean π^0 signal, the significance of the B_d signal was found to be satisfying (≈ 60).

Acknowledgements

This work has been performed within the ATLAS Collaboration and we have made use of the software framework and tools which are the result of collaboration-wide efforts. We thank collaboration members for the helpful discussions with special acknowledgements to Johann Collot, David Rousseau and Monika Wielers for reading, commenting and making suggestions to improve this note.

References

[1] R. Fleischer, CERN-TH/99-78, hep-ph/9903455.

[2] P.Z. Skands, Int. J. High Energy Phys. 0101 (2001) 8, hep-ph/0010115

[3] T. Sjöstrand, PYTHIA 5.7 and Jetset 7.4, hep-ph/9508391 and Computer Physics Commun. 82 (1994) 74.
see also the ATLAS B physics simulation web Page: http://msmizans.home.cern.ch/msmizans/production/0.html .

[4] S. Simion, ATLAS note: ATL-SOFT-99-001

[5] CBN-Tuples: http://droussea.home.cern.ch/droussea/cbnt/cbnt.html

[6] Review of Particle Physics, Europ. Phys. Journ. C 15,(2000) 1-4.

[7] C. Driouichi, P. Eerola, M. Melcher, F. Ohlsson-Malek and S. Viret, scientific note in preparation, 2001.

[8] J/ψ reconstruction in the inner detector, S. Viret, rapport de stage DEA, matière et rayonnement, 2001.

[9] M.Wielers, ATLAS note: ATL-PHYS-99-016

[10] K_S^0 reconstruction in the ATLAS Inner Detector, J. Damet, G.F. Tartarelli; ATL-INDET-99-024